The lipid 5-phoshatase SHIP2 controls renal brush border ultrastructure and function by regulating the activation of ERM proteins

Sufyan G. Sayyed[1], François Jouret[2], Marjorie Vermeersch[3], David Pérez-Morga[3,4] and Stéphane Schurmans[1]

[1]Laboratoire de Génétique Fonctionnelle, GIGA-B34, Université de Liège, Liège, Belgium; [2]Experimental Surgery, GIGA Cardiovascular Sciences, Université de Liège, Liège, Belgium; [3]Center for Microscopy and Molecular Imaging (CMMI), Université Libre de Bruxelles, Gosselies, Belgium; and [4]Laboratoire de Parasitologie Moléculaire, Institut de Biologie et de Médecine Moléculaires (IBMM), Université Libre de Bruxelles, Gosselies, Belgium

The microvillus brush border on the renal proximal tubule epithelium allows the controlled reabsorption of solutes that are filtered through the glomerulus and thus participates in general body homeostasis. Here, using the lipid 5-phosphatase *Ship2* global knockout mice, proximal tubule–specific *Ship2* knockout mice, and a proximal tubule cell model in which SHIP2 is inactivated, we show that SHIP2 is a negative regulator of microvilli formation, thereby controlling solute reabsorption by the proximal tubule. We found increased PtdIns(4,5)P2 substrate and decreased PtdIns4P product when SHIP2 was inactivated, associated with hyperactivated ezrin/radixin/moesin proteins and increased Rho-GTP. Thus, inactivation of SHIP2 leads to increased microvilli formation and solute reabsorption by the renal proximal tubule. This may represent an innovative therapeutic target for renal Fanconi syndrome characterized by decreased reabsorption of solutes by this nephron segment.

Kidney International (2017) **92,** 125–139; http://dx.doi.org/10.1016/j.kint.2017.01.008

KEYWORDS: Fanconi syndrome; microvilli; phosphoinositide; proximal tubule; renal brush border; Ship2/Inppl1

The renal proximal tubule (PT) plays an essential role in the control of body homeostasis because this nephron segment, which lies just downstream of the glomerulus where blood is filtered to generate the primary urine, is responsible for controlled reabsorption of solutes. In normal conditions, filtered glucose, amino acids, phosphate, potassium, sodium, water, and low molecular weight proteins (LMWPs) are reabsorbed by PT cells. LMWPs are taken up by a complex megalin-cubilin receptor–mediated endocytic pathway, whereas solutes use active or passive transport through channels and transporters. The epithelial cells lining the PT exhibit a number of structural features indicative of a tissue involved in intense reabsorption processes. Probably the most important feature is the presence of extensive microvilli creating a so-called brush border at the luminal pole of the PT epithelium. This enlargement of the luminal membrane markedly increases the reabsorption surface, facilitating the endocytosis of macromolecules and the transport of solutes. The physiologic importance of such a reabsorption process is underscored by the pathologic and clinical changes observed in patients with renal Fanconi syndrome. This condition of acquired or inherited PT dysfunction is associated with an increased urinary loss of essential metabolites and LMWPs, thereby leading to polyuria, polydipsia and dehydration, hypokalemia, acidosis, impaired growth, and osteomalacia.[1–3]

Factors controlling the renal brush border ultrastructure and function are not well characterized *in vivo*. The lipid 5-phosphatase SHIP2 (also known as INPPL1) is well expressed in the adult kidney,[4,5] but its function *in vivo* in this tissue is unknown. Our *in vivo* and *in vitro* studies highlight the essential but unexpected role of this phosphatase in the control of the formation of microvilli and PT function and suggest that the enzyme could represent a novel therapeutic target for renal Fanconi syndrome.

Correspondence: *Stéphane Schurmans, Laboratoire de Génétique Fonctionnelle, GIGA-B34, Université de Liège, Avenue de l'Hôpital 11, 4000 Liège, Belgium. E-mail: sschurmans@ulg.ac.be*

Received 18 August 2016; revised 1 January 2017; accepted 6 January 2017; published online 13 March 2017

RESULTS

The SHIP2 protein is expressed in the renal PT

Ship2 mRNA has been previously detected in mouse embryonic and adult kidney by *in situ* hybridization and semi-quantitative reverse transcriptase polymerase chain reaction,

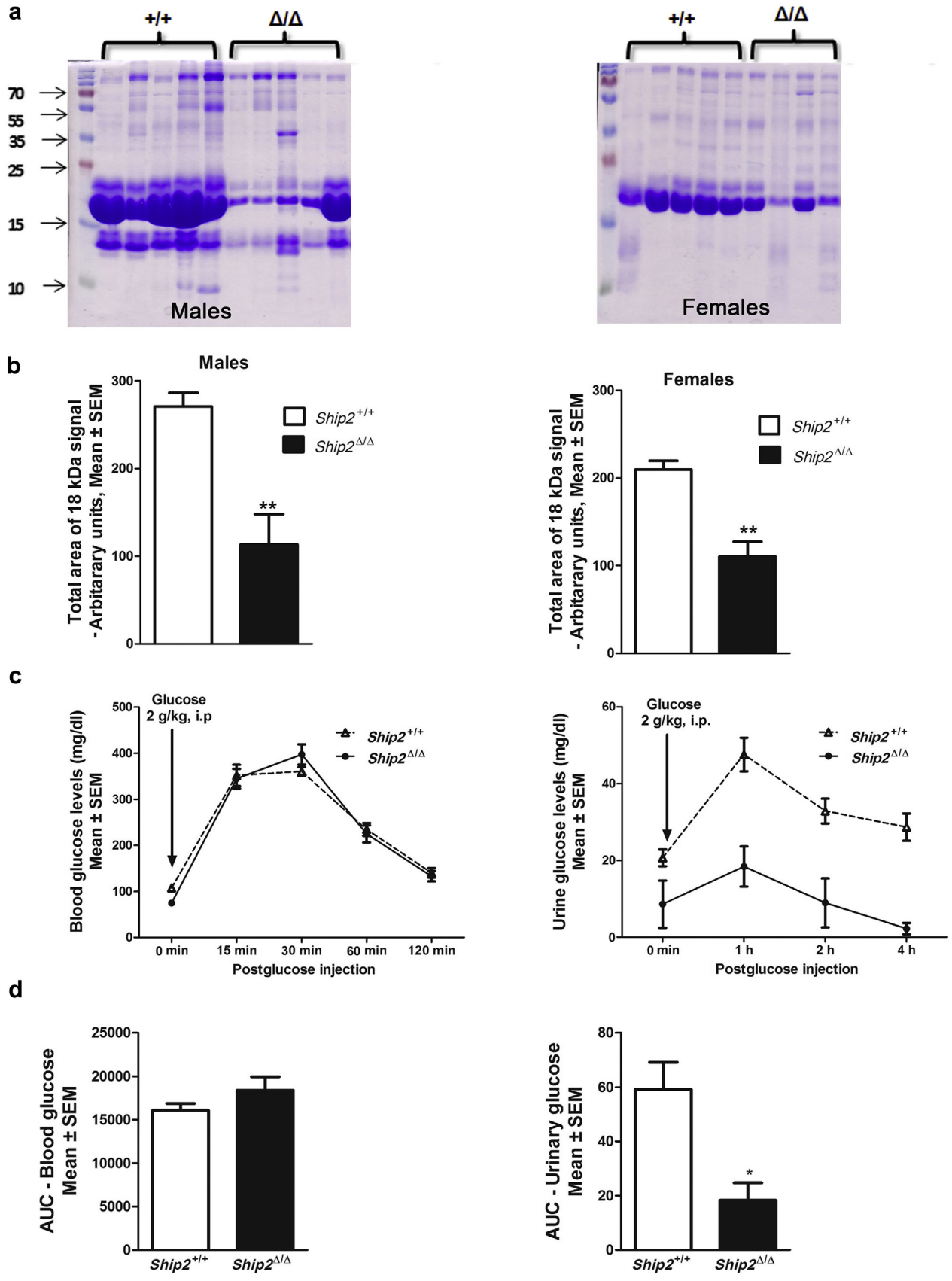
a
+/+
Δ/Δ
70
55
35
25
15
10
Males
Females
b
Males
Total area of 18 kDa signal - Arbitrary units, Mean ± SEM
Ship2+/+
Ship2Δ/Δ
**
Females
c
Glucose 2 g/kg, i.p
Blood glucose levels (mg/dl) Mean ± SEM
0 min
15 min
30 min
60 min
120 min
Postglucose injection
Urine glucose levels (mg/dl) Mean ± SEM
1 h
2 h
4 h
d
AUC - Blood glucose Mean ± SEM
AUC - Urinary glucose Mean ± SEM
*

but no data are currently available on SHIP2 protein expression in the mouse renal PT.[4,5] Analysis of SHIP2 expression by immunodetection on a kidney protein extract revealed a signal at ~140 kDa, the expected size for SHIP2 protein (Supplementary Figure S1A). On kidney sections, a widespread SHIP2 expression was observed by immunofluorescence (IF). In the renal cortex, both glomeruli and surrounding tubules were positive for SHIP2 (Supplementary Figure S1B). Megalin, a component of the endocytic receptor complex in the renal PT brush border, colocalized in SHIP2-positive cells (Supplementary Figure S1C and D). Together, our results indicate that SHIP2 is well expressed in kidneys and is particularly abundant in PT cells.

Urine analyses suggest an increased function of reabsorption by the renal PT in *Ship2*$^{\Delta/\Delta}$ mice

The general kidney function was assessed in female and male *Ship2*$^{+/+}$ and *Ship2*$^{\Delta/\Delta}$ full knockout mice by measuring the glomerular filtration rate (GFR). No significant difference was observed in the GFR between the groups of female and male mice whether or not GFR was normalized to body weight or kidney weight (Supplementary Table S1). Next, plasma creatinine levels were analyzed in female and male *Ship2*$^{+/+}$ and *Ship2*$^{\Delta/\Delta}$ mice (Supplementary Table S1). No significant difference was observed in plasma creatinine levels between these groups. Finally, urinary LMWP and glucose excretion analyses were performed in order to more specifically address the function of reabsorption by the PT. First, the protein profile was analyzed in the urine of female and male mice by sodium dodecylsulfate polyacrylamide gel electrophoresis (Figure 1a). Proteins with a molecular weight <25 kDa were markedly decreased in the urine of *Ship2*$^{\Delta/\Delta}$ mice compared with *Ship2*$^{+/+}$ mice. Quantification of the major protein signal at ~18 kDa, most probably odorant-binding proteins belonging to the lipocalin superfamily,[6–8] confirmed that significantly lower levels were present in female and male *Ship2*$^{\Delta/\Delta}$ mice compared with *Ship2*$^{+/+}$ mice (Figure 1b). Second, urinary glucose excretion was analyzed in mice after i.p. injection of 2 g of glucose per kilogram of body weight (Figure 1c and d). A significantly lower amount of glucose was found over a 4-hour period in the urine of *Ship2*$^{\Delta/\Delta}$ mice compared with *Ship2*$^{+/+}$ mice. No significant difference was observed in plasma glucose concentrations between the 2 groups of mice over a 2-hour period.

Together, our results indicate that *Ship2*$^{\Delta/\Delta}$ mice have normal GFR and plasma creatinine levels associated with decreased urinary levels of LMWP and injected glucose. These alterations suggest that *Ship2* catalytic inactivation in mice leads to increased function of reabsorption by the renal PT.

Structural and ultrastructural alterations in the *Ship2*$^{\Delta/\Delta}$ PT

Macroscopically, kidneys from 20-week-old female and male *Ship2*$^{\Delta/\Delta}$ mice were smaller than those from age- and sex-matched *Ship2*$^{+/+}$ mice (Supplementary Table S1). Microscopically, no obvious alteration was observed in *Ship2*$^{\Delta/\Delta}$ kidney sections stained with hematoxylin and eosin compared with *Ship2*$^{+/+}$ sections (Supplementary Figure S2A and B). In particular, glomeruli and tubule density as well as the general structure of the kidney were found to be normal (Supplementary Figure 2C). Because urine analyses in *Ship2*$^{\Delta/\Delta}$ mice point to potential PT abnormalities, this nephron section was analyzed by IF with a megalin antibody (Figure 2a). Megalin expression was markedly increased in kidney sections from *Ship2*$^{\Delta/\Delta}$ mice compared with *Ship2*$^{+/+}$ mice. Immunodetection on kidney protein extracts with the same megalin antibody confirmed these IF results: the megalin signal was significantly increased in *Ship2*$^{\Delta/\Delta}$ kidneys compared with *Ship2*$^{+/+}$ kidneys (Figure 2b). At the mRNA level, a slight but significant increase in expression was observed for megalin in *Ship2*$^{\Delta/\Delta}$ kidneys compared with *Ship2*$^{+/+}$ kidneys (Supplementary Figure S3A and Supplementary Table S2). Expression levels of mRNA coding for cubilin, Sglt2, and Clcn5, all proteins expressed in the PT brush border, were also significantly increased in *Ship2*$^{\Delta/\Delta}$ kidneys (Supplementary Figures S3B–D). By contrast, expression levels of mRNA coding for OCT1, OCT2, and Slc22a26 proteins localized at the basolateral membrane of PT cells were not altered for except of OAT1, which was found to be significantly decreased in *Ship2*$^{\Delta/\Delta}$ compared with *Ship2*$^{+/+}$ kidneys (Supplementary Figure S3E–H).

Scanning electron microscopy (SEM) analysis revealed major alterations in *Ship2*$^{\Delta/\Delta}$ PTs (Figure 2c and d). On longitudinal sections, the PT appeared much more convoluted or distorted on the lumen side in *Ship2*$^{\Delta/\Delta}$ mice due to large epithelial protrusions into the lumen compared with *Ship2*$^{+/+}$ mice (Figure 2c). Some microvilli were abnormally elongated in the *Ship2*$^{\Delta/\Delta}$ brush border and sometimes made a bridge between 2 opposing PT cells. Those abnormal microvilli and bridges of microvilli were not observed in *Ship2*$^{+/+}$ mice. The intrusion of the PT brush border into the Bowman capsule was much more prominent in *Ship2*$^{\Delta/\Delta}$ mice compared with

Figure 1 | Urine analysis in *Ship2*$^{+/+}$ and *Ship2*$^{\Delta/\Delta}$ mice. (**a,b**) Urinary protein profile was analyzed in male (left panel) and female (right panel) 20-week-old mice. Urine volumes, normalized to total urinary protein levels, were loaded onto a nonreducing sodium dodecylsulfate polyacrylamide gel followed by staining with Coomassie blue. Marker proteins are shown. Proteins with a molecular weight <25 kDa were markedly decreased in the urine of *Ship2*$^{\Delta/\Delta}$ mice compared with *Ship2*$^{+/+}$ mice. (**b**) Quantification of the major protein signal at ~18 kDa was performed in males (left panel) and females (right panel) using ImageJ software (NIH). Statistics (Student's *t* test): $^{**}P < 0.01$ compared with *Ship2*$^{+/+}$ mice. (**c,d**) Twenty-week-old mice (7–17 per genotype) were i.p. injected with 2 g of glucose per kilogram of body weight. The mean ± SEM of glucose in blood (left panel) and urine (right panel) was analyzed over 2- and 4-hour periods, respectively. A significantly lower amount of glucose was found over a 4-hour period in the urine of *Ship2*$^{\Delta/\Delta}$ mice compared with *Ship2*$^{+/+}$ mice. (**d**) The areas under the curve (AUC) were determined using Graph Pad Prism software. Statistics (Student's *t* test): $^{*}P < 0.05$ compared with *Ship2*$^{+/+}$ mice. To optimize viewing of this image, please see the online version of this article at www.kidney-international.org.

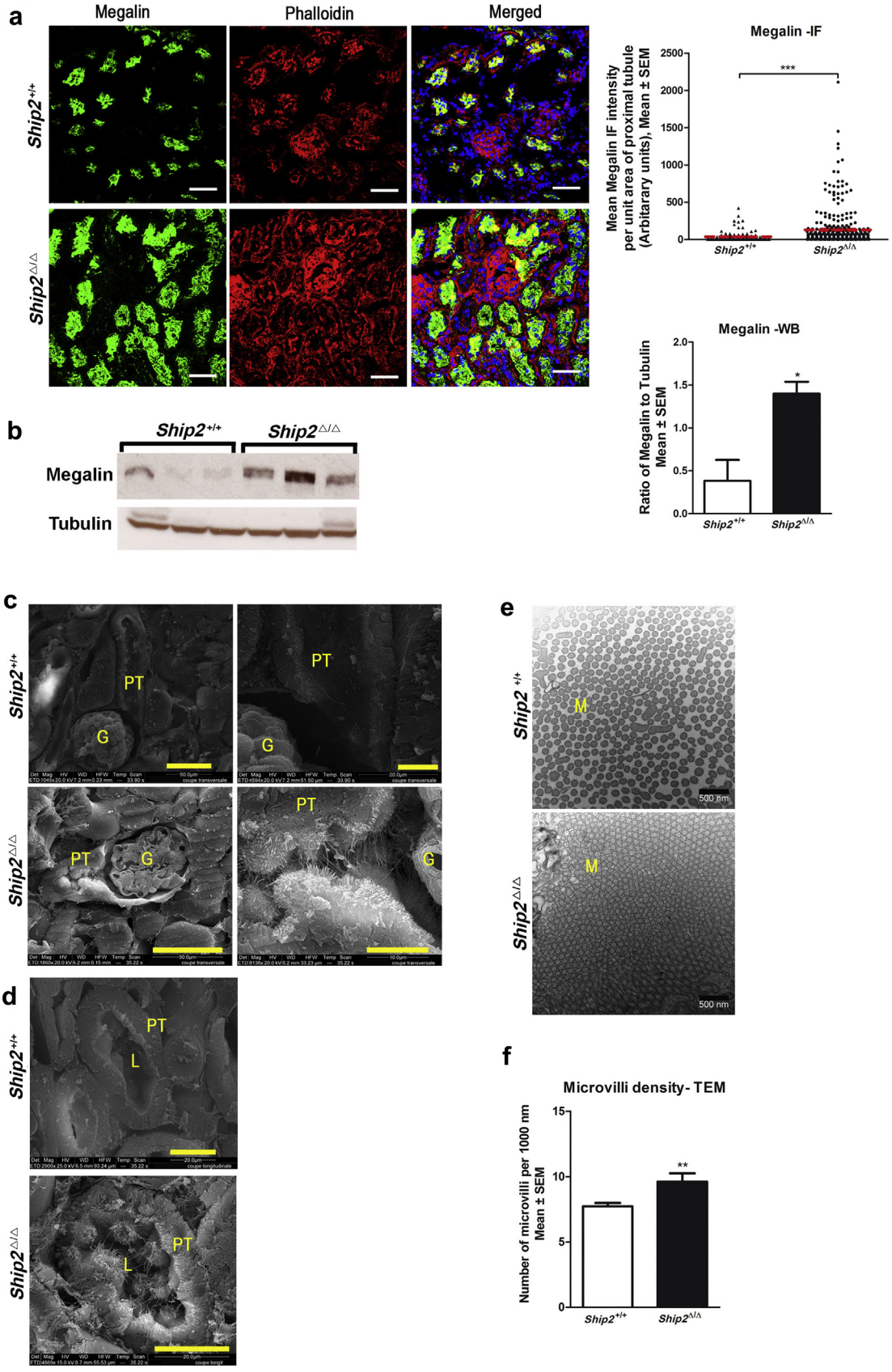
a
Megalin
Phalloidin
Merged
Ship2+/+
Ship2△/△
Megalin -IF
Mean Megalin IF intensity per unit area of proximal tubule (Arbitrary units), Mean ± SEM
2500
2000
1500
1000
500
0
***
Ship2+/+
Ship2Δ/Δ
b
Ship2+/+
Ship2△/△
Megalin
Tubulin
Megalin -WB
Ratio of Megalin to Tubulin Mean ± SEM
2.0
1.5
1.0
0.5
0.0
*
Ship2+/+
Ship2Δ/Δ
c
Ship2+/+
Ship2△/△
PT
G
d
Ship2+/+
Ship2△/△
PT
L
e
Ship2+/+
Ship2△/△
M
500 nm
f
Microvilli density- TEM
Number of microvilli per 1000 nm Mean ± SEM
15
10
5
0
**
Ship2+/+
Ship2Δ/Δ

Ship2$^{+/+}$ mice. The invasion of the Bowman capsule by such an abnormal PT brush border was particularly obvious when viewed from the glomerulus side (Figure 2c). Transmission electron microscopy analysis revealed that microvilli in *Ship2*$^{+/+}$ mice were well separated from each other by a space, whereas in *Ship2*$^{\Delta/\Delta}$ mice, they were densely packed against each other without any space to separate them, significantly increasing their density (Figure 2e and f). Microvilli thickness was similar in *Ship2*$^{+/+}$ and *Ship2*$^{\Delta/\Delta}$ mice (Supplementary Figure S4).

Together, our results indicate that catalytic inactivation of SHIP2 leads to increased density of microvilli on PT cells and a more pronounced invasion of the Bowman capsule by this abnormal brush border. Some microvilli in *Ship2*$^{\Delta/\Delta}$ mice appeared abnormally elongated and connected 2 opposing PT cells. Finally, the increased density of microvilli on *Ship2*$^{\Delta/\Delta}$ PT cells was associated with increased expression of megalin and other microvillus components, with no significant change on the basolateral side.

Structural, ultrastructural, and functional alterations in mice with a SHIP2 inactivation specifically in PT cells

In order to investigate whether SHIP2 catalytic inactivation specifically in PT cells is sufficient to recapitulate the phenotype observed in *Ship2*$^{\Delta/\Delta}$ kidneys, we used mouse sodium/glucose transporter-2 (mSglt2-Cre) mice that express the Cre recombinase in PT cells to generate and analyze *Ship2*$^{flox/flox}$ mSglt2-Cre mice.[9] IF analysis of *Ship2*$^{flox/flox}$ mSglt2-Cre kidney sections revealed, as expected, that the SHIP2 signal was still present in phalloidin-positive PT cells, but somewhat decreased compared with phalloidin-positive PT of control kidneys (Supplementary Figure S5). Indeed, in our *Ship2* genetically modified mouse, the *Ship2*$^{\Delta}$ allele still produces a slightly unstable, catalytically inactive, truncated SHIP2 protein that is recognized by the Ship2 antibody.[10] Macroscopically, 20-week-old male and female *Ship2*$^{flox/flox}$ mSglt2-Cre mice had normal body and kidney weights compared with age- and sex-matched *Ship2*$^{+/+}$ mSglt2-Cre, *Ship2*$^{+/flox}$, and *Ship2*$^{flox/flox}$ mice, all referred as control mice (Supplementary Table S3). These *Ship2*$^{flox/flox}$ mSglt2-Cre mice did not present the characteristic facial dysmorphy observed in *Ship2*$^{\Delta/\Delta}$ mice and were of normal length (Supplementary Figure S6A). Microscopically, no obvious alteration was observed in *Ship2*$^{flox/flox}$ mSglt2-Cre kidney sections stained with hematoxylin and eosin compared with control kidney sections (Supplementary Figure S6B). Megalin expression was significantly increased in kidney sections from *Ship2*$^{flox/flox}$ mSglt2-Cre mices compared with control mice (Figure 3a). SEM analysis revealed major alterations in *Ship2*$^{flox/flox}$ mSglt2-Cre PTs, very similar to those observed in *Ship2*$^{\Delta/\Delta}$ mice (Figure 3b). Indeed, large epithelial protrusions into the PT lumen and some abnormally elongated microvilli were observed in *Ship2*$^{flox/flox}$ mSglt2-Cre mice; some microvilli made a bridge between 2 opposing PT cells (Figure 3b). The intrusion of the PT brush border into the Bowman capsule was also more prominent in *Ship2*$^{flox/flox}$ mSglt2-Cre mice compared with control mice but less severe than in *Ship2*$^{\Delta/\Delta}$ mice (Figure 3c). A major difference with *Ship2*$^{\Delta/\Delta}$ mice was the presence of the PT and brush borders with only slight alterations in *Ship2*$^{flox/flox}$ mSglt2-Cre mice (Supplementary Figure S6C). *Ship2*$^{flox/flox}$ mSglt2-Cre mice had a normal GFR/kidney weight and plasma creatinine level, but increased urinary creatinine levels compared with control mice (Supplementary Table S3). Urinary protein analysis showed decreased signals corresponding to proteins with a molecular weight <25 kDa in some male and female *Ship2*$^{flox/flox}$ mSglt2-Cre mice compared with control mice (Figure 4a). Quantification of the major protein signal at ~18 kDa, most probably odorant-binding proteins belonging to the lipocalin superfamily,[6–8] confirmed that there was a trend toward lower levels in *Ship2*$^{flox/flox}$ mSglt2-Cre mice than in control mice (Figure 4b). Urinary albumin excretion was specifically addressed after i.v. injection of fluorescein isothiocyanate (FITC)-albumin into *Ship2*$^{flox/flox}$ mSglt2-Cre and control mice (Figure 4c). One hour after injection, a trend toward decreased urinary fluorescence intensity was observed in *Ship2*$^{flox/flox}$ mSglt2-Cre mice compared with control mice. Fractional renal excretion of phosphate and urinary osmolarity were significantly decreased in *Ship2*$^{flox/flox}$ mSglt2-Cre mice compared with control mice (Figure 4d and e). Finally, urinary glucose excretion was analyzed in *Ship2*$^{flox/flox}$ mSglt2-Cre and control mice after i.p. injection of 2 g of glucose per kilogram of body weight (Figure 4f). A trend toward a lower amount of glucose was found over a 4-hour period in the urine of

Figure 2 | Structural and ultrastructural alterations in *Ship2*$^{\Delta/\Delta}$ renal proximal tubules. (**a**) Immunofluorescence analysis of *Ship2*$^{+/+}$ and *Ship2*$^{\Delta/\Delta}$ kidney sections (5 μm) with a megalin antibody (green) and phalloidin (red). Bars = 50 μm. The graph represents the quantification of the megalin signal per unit area of a proximal tubule (PT); the mean immunofluorescence (IF) intensity ± SEM are shown. At least 100 PTs were analyzed per genotype; each dot represents a PT (**b**) immunodetection on kidney protein extracts from three 20-week-old *Ship2*$^{+/+}$ and *Ship2*$^{\Delta/\Delta}$ mice with megalin and tubulin antibodies. The graph represents the mean ± SEM of the ratio of megalin over tubulin signals for each genotype. Megalin expression was markedly increased in kidney sections from *Ship2*$^{\Delta/\Delta}$ mice compared with *Ship2*$^{+/+}$ mice. Statistics (Student's *t* test): **P* < 0.05 compared with *Ship2*$^{+/+}$ mice. (**c**) SEM analysis of longitudinal sections from *Ship2*$^{+/+}$ and *Ship2*$^{\Delta/\Delta}$ PTs. G, glomerulus. The PTs appeared much more convoluted or distorted on the lumen side in *Ship2*$^{\Delta/\Delta}$ mice due to large epithelial protrusions into the lumen compared with *Ship2*$^{+/+}$ mice. Bars = 50 μm in the panels on the left and 10 μm in the panels on the right. (**d**) SEM analysis of kidney sections from *Ship2*$^{+/+}$ and *Ship2*$^{\Delta/\Delta}$ mice: the PT orifice is seen from the glomerulus. Bars = 20 μm. (**e**) Transmission electron microscopy analysis of transverse sections from *Ship2*$^{+/+}$ and *Ship2*$^{\Delta/\Delta}$ brush borders. Bars = 500 nm. (**f**) The graph represents the number of microvilli crossing a 1-μm-long line drawn on the PT transverse sections shown in (**e**), as a measure of microvilli density in PT cells from *Ship2*$^{+/+}$ and *Ship2*$^{\Delta/\Delta}$ brush borders. Statistics (Student's *t* test): ***P* < 0.01. To optimize viewing of this image, please see the online version of this article at www.kidney-international.org.

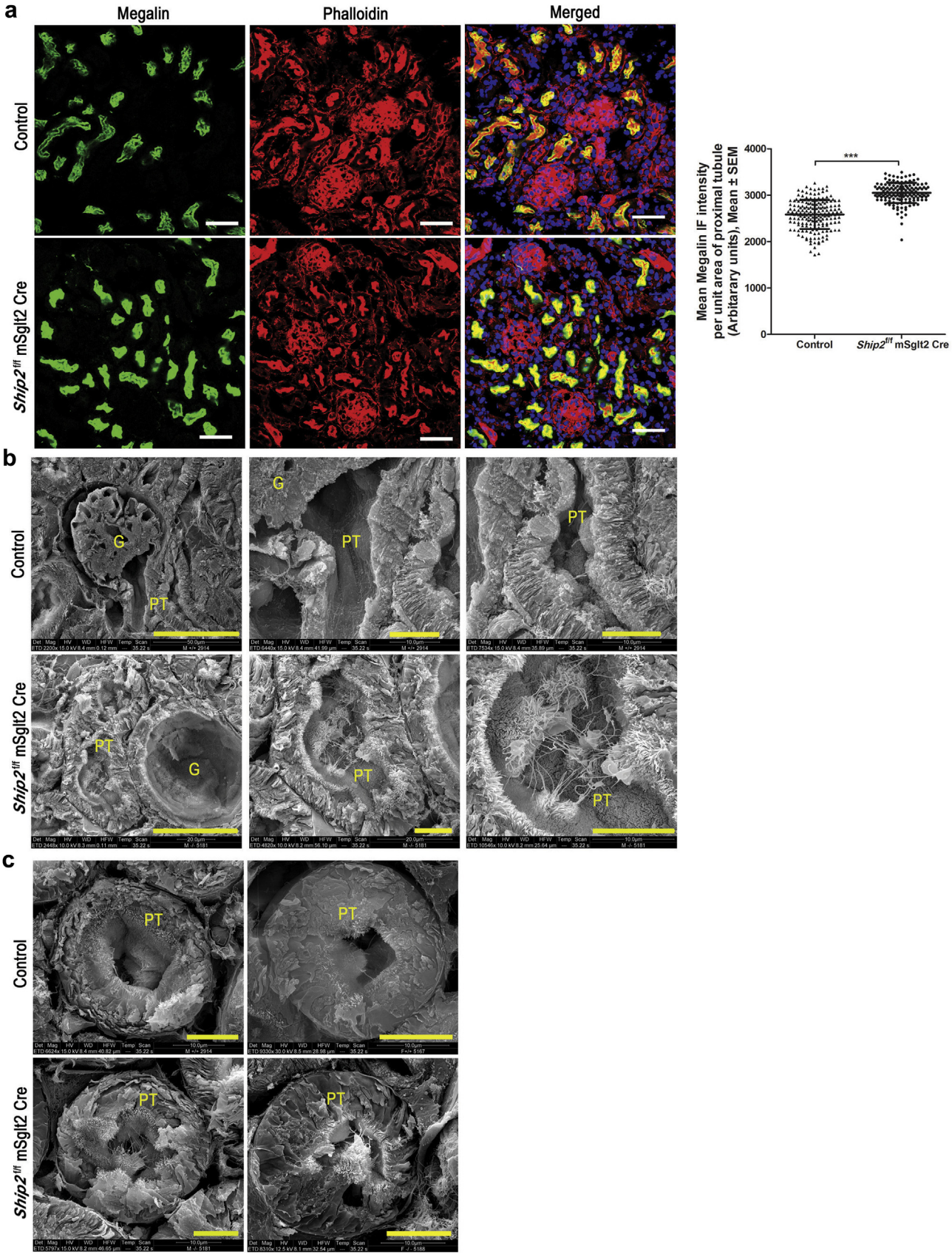
a
Megalin
Phalloidin
Merged
Control
Ship2f/f mSglt2 Cre
Mean Megalin IF intensity per unit area of proximal tubule (Arbitrary units), Mean ± SEM
4000
3000
2000
1000
0
***
Control
Ship2f/f mSglt2 Cre
b
Control
Ship2f/f mSglt2 Cre
G
PT
c
Control
Ship2f/f mSglt2 Cre
PT

Ship2$^{flox/flox}$ mSglt2-Cre mice compared with control mice. No significant difference was observed in plasma glucose concentrations between the 2 groups of mice over a 2-hour period.

Together, our results indicate that SHIP2 catalytic inactivation specifically in PT cells confirms most of *Ship2*$^{\Delta/\Delta}$ structural, ultrastructural, and functional kidney alterations defined earlier. However, PTs with slight or no obvious SEM/transmission electron microscopy alterations were also present in *Ship2*$^{flox/flox}$ mSglt2-Cre mice, suggesting an incomplete penetrance of the phenotype when using mSglt2-Cre mice (Supplementary Figure S6C). Structural and ultrastructural alterations in *Ship2*$^{flox/flox}$ mSglt2-Cre mice were associated with a trend toward decreased urinary levels of LMWP and injected FITC-albumin or glucose. Significant reductions in fractional excretion of phosphate and urinary osmolarity were observed in *Ship2*$^{flox/flox}$ mSglt2-Cre mice, indicating that reabsorption by PTs is increased in these mice compared with control mice.

SHIP2 inactivation in the pig LLC-PK1 PT cell line confirms structural, ultrastructural, and functional alterations observed in *Ship2*$^{\Delta/\Delta}$ and *Ship2*$^{flox/flox}$ mSglt2-Cre PTs

In agreement with previous reports,[11,12] microvilli were detected by SEM on confluent cultures of the pig LLC-PK1 PT cell line (Figure 5a). IF analysis showed that SHIP2 was mainly expressed in the cytoplasm of LLC-PK1 cells up to and sometimes including the basis of phalloidin- and ezrin-positive microvilli (Figure 5b, Supplementary Figure S7). SEM analysis of confluent LLC-PK1 cell cultures treated with 5 or 10 μM SHIP2 catalytic inhibitor revealed increased density of microvilli (Figure 5c). Accordingly, expression of phalloidin, ezrin, and megalin in microvilli was significantly increased in SHIP2 catalytic inhibitor–treated LLC-PK1 cell cultures compared with dimethylsulfoxide (DMSO)-treated cell cultures (Figure 5d, Supplementary Figure S8A). Functionally, FITC-albumin uptake by microvilli from confluent LLC-PK1 cell cultures was significantly increased in the presence of 10 μM SHIP2 catalytic inhibitor compared with DMSO-treated LLC-PK1 cells (Figure 5e, Supplementary Figure S8B). Finally, transduction of LLC-PK1 cells with lentivirus expressing *Ship2*-specific small, interfering RNAs (siRNAs) also resulted in increased phalloidin expression in microvilli compared with scrambled siRNAs (Supplementary Figures S9 and S10).

Together, our results indicate that SHIP2 inactivation in confluent pig LLC-PK1 PT cells leads to increased density of microvilli; expression of phalloidin, ezrin, and megalin in microvilli; and FITC-albumin uptake. This cellular model confirms most of the PT-cell alterations found in mice with SHIP2 inactivation and is thus relevant to study the mechanism of SHIP2 action on the formation of microvilli.

PtdIns(4,5)P2, PtdIns4P, phospho-ezrin/radizin/moesin proteins, and RhoA-GTP levels in LLC-PK1 cells after SHIP2 inactivation

PtdIns(4,5)P2 is both a SHIP2 substrate and a direct activation signal for ezrin/radixin/moesin (ERM) proteins, which play an important role in the formation of microvilli in *in vitro* and *in vivo* models.[13–17] IF analysis of confluent LLC-PK1 cells revealed that the plasma membrane/microvilli PtdIns(4,5)P2 signal is significantly higher in cells treated with 5 or 10 μM SHIP2 inhibitor than with DMSO (Figure 6a). Conversely, the plasma membrane/microvilli PtdIns4P signal, which is the product of the SHIP2 action on PtdIns(4,5)P2, was significantly lower in 5- or 10-μM SHIP2 inhibitor–treated cells than in DMSO-treated cells (Figure 6b). Because PtdIns(4,5)P2 binds and activates ERM proteins, active phospho-ERM (p-ERM) proteins were next investigated in LLC-PK1 cells by IF. Both the p-ERM signal and the ratio of p-ERM signal to ezrin signal were significantly higher in LLC-PK1 cells treated with 5 or 10 μM SHIP2 inhibitor than with DMSO (Figure 6c). Interestingly, immunodetection of p-ERM by Western blotting on kidney protein extracts showed a stronger p-ERM signal in *Ship2*$^{\Delta/\Delta}$ than in *Ship2*$^{+/+}$ mice, supporting the IF results obtained in LLC-PK1 cells (Supplementary Figure S11). p-ERM proteins not only participate in the formation of microvilli in different models, but also activate Rho in a positive feedback cycle to amplify a signal pathway, further activating ERM proteins and the formation of microvilli.[13,16–20] Active RhoA-GTP was thus investigated in LLC-PK1 cells using IF; the RhoA-GTP signal was found to be significantly increased in LLC-PK1 cells treated with 10 μM SHIP2 inhibitor compared with DMSO-treated LLC-PK1 cells, and a trend toward increased RhoA-GTP signal was observed in 5-μM SHIP2 inhibitor–treated LLC-PK1 cells (Figure 6d). Because Rho-GTP is known to activate PtdIns4P 5-kinase (PIP5K) to produce PtdIns(4,5)P2, which in turn activates ERM proteins and closes the positive feedback cycle,[19,20] the effect of PIP5K1b transfection was investigated in LLC-PK1 cells treated or not with the SHIP2 catalytic inhibitor. As expected, expression of Myc-tagged PIP5K1b in DMSO-treated LLC-PK1 cells induced

Figure 3 | Structural and ultrastructural alterations in *Ship2*$^{flox/flox}$ mSglt2-Cre renal proximal tubules. (**a**) Immunofluorescence (IF) analysis of *Ship2*$^{flox/flox}$ mSglt2-Cre and control kidney sections (5 μm) with a megalin antibody (green) and phalloidin (red). Bars = 50 μm. The graph shows the mean megalin IF intensity per unit of proximal tubule (PT) area. At least 100 PTs were analyzed per genotype; each dot represents a PT. Megalin expression was significantly increased in kidney sections from *Ship2*$^{flox/flox}$ mSglt2-Cre mice compared with control mice. Statistics (Student's *t* test): ***$P < 0.001$. (**b**) SEM analysis of longitudinal sections from *Ship2*$^{flox/flox}$ mSglt2-Cre and control PTs. Large epithelial protrusions into the PT lumen and some abnormally elongated microvilli were observed in *Ship2*$^{flox/flox}$ mSglt2-Cre mice. G, glomerulus. Bars = 50 μm in the panel on the left and 10 μm in the panels in the middle and on the right. (**c**) SEM analysis of kidney sections from *Ship2*$^{flox/flox}$ mSglt2-Cre and control mice: the PT orifice is seen from the glomerulus. Bars = 10 μm. To optimize viewing of this image, please see the online version of this article at www.kidney-international.org.

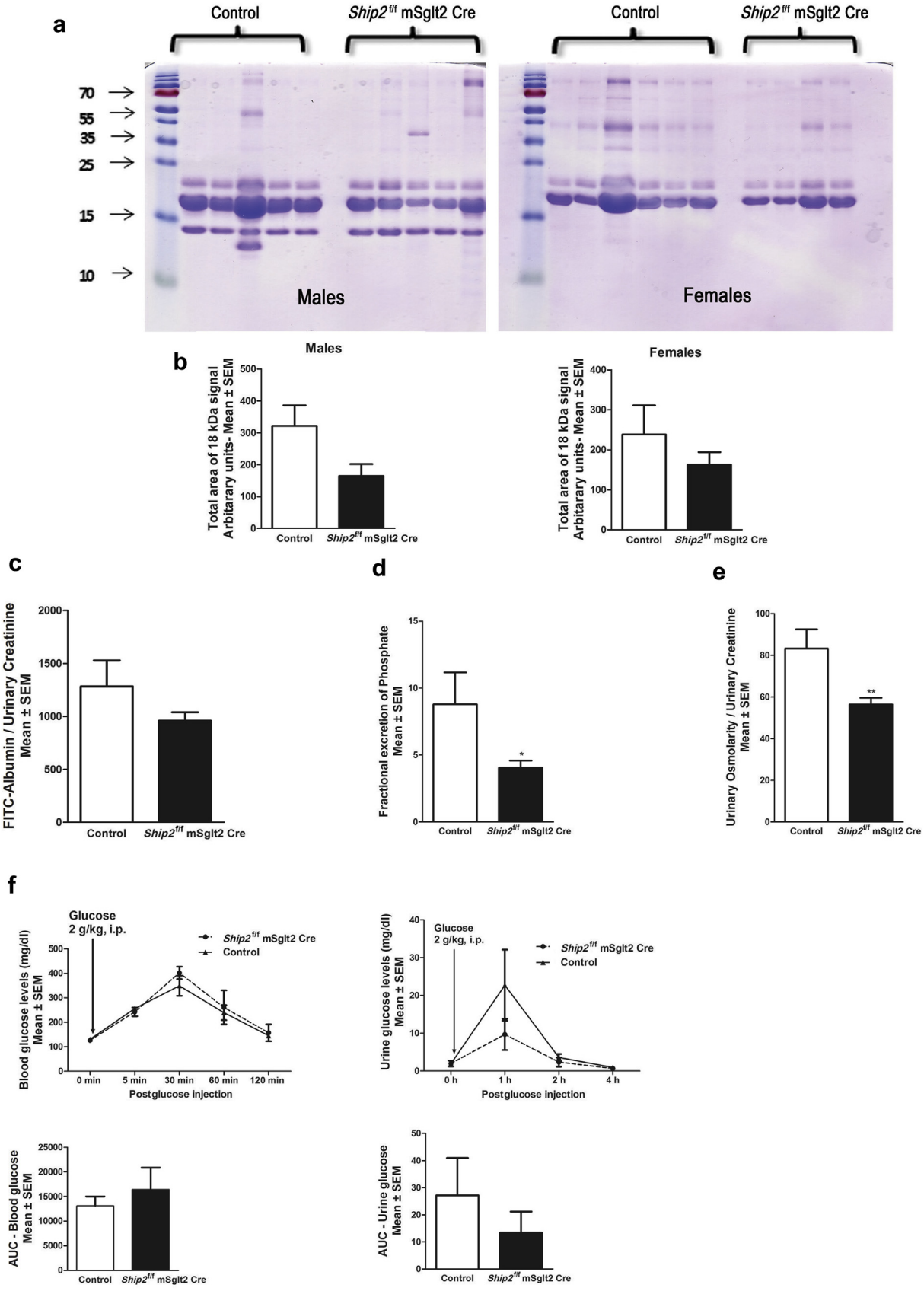
a
Control
Ship2f/f mSglt2 Cre
Control
Ship2f/f mSglt2 Cre
70
55
35
25
15
10
Males
Females
b
Males
Total area of 18 kDa signal Arbitrary units- Mean ± SEM
Control
Ship2f/f mSglt2 Cre
Females
Total area of 18 kDa signal Arbitrary units- Mean ± SEM
Control
Ship2f/f mSglt2 Cre
c
FITC-Albumin / Urinary Creatinine Mean ± SEM
Control
Ship2f/f mSglt2 Cre
d
Fractional excretion of Phosphate Mean ± SEM
Control
Ship2f/f mSglt2 Cre
e
Urinary Osmolarity / Urinary Creatinine Mean ± SEM
Control
Ship2f/f mSglt2 Cre
f
Glucose 2 g/kg, i.p.
Ship2f/f mSglt2 Cre
Control
Blood glucose levels (mg/dl) Mean ± SEM
0 min
5 min
30 min
60 min
120 min
Postglucose injection
Glucose 2 g/kg, i.p.
Ship2f/f mSglt2 Cre
Control
Urine glucose levels (mg/dl) Mean ± SEM
0 h
1 h
2 h
4 h
Postglucose injection
AUC - Blood glucose Mean ± SEM
Control
Ship2f/f mSglt2 Cre
AUC - Urine glucose Mean ± SEM
Control
Ship2f/f mSglt2 Cre

significant increased plasma membrane/microvilli PtdIns(4,5)P2 levels and Phalloidin signals compared with neighboring nontransfected LLC-PK1 cells (Figure 7a and b, upper 4 panels [DMSO]). Then, LLC-PK1 cells transfected with Myc-tagged PIP5K1b were treated with 5 or 10 μM SHIP2 catalytic inhibitor. We found that the plasma membrane/microvilli PtdIns(4,5)P2 level and phalloidin signal were further increased in SHIP2 inhibitor–treated LLC-PK1 cells transfected with PIP5K1b compared with neighboring nontransfected SHIP2 catalytic inhibitor-treated LLC-PK1 cells (Figure 7a and b). Finally, transduction of LLC-PK1 cells with lentivirus expressing *Ship2*-specific siRNAs also resulted in a significant increase p-ERM expression in microvilli compared with scrambled siRNAs (Supplementary Figure S10A and B). The increased formation of microvilli in those transduced cells was associated with increased PtdIns(4,5)P2 levels (Supplementary Figure S10C and D).

Together, our results indicate that SHIP2 inactivation in confluent pig LLC-PK1 PT cells leads to increased plasma membrane/microvilli PtdIns(4,5)P2 substrate, decreased PtdIns4P product, and increased active p-ERM proteins and RhoA-GTP levels.

DISCUSSION

The renal PT brush border plays an essential role in body homeostasis because it is responsible for the controlled reabsorption of specific solutes that have been filtered through the glomerulus. However, the molecular mechanisms controlling brush border formation of microvilli on PT epithelial cells are still largely unknown. In this study, we show that the lipid 5-phosphatase SHIP2 is a negative regulator of the formation of microvilli in PT, probably acting by dephosphorylating PtdIns(4,5)P2 in PtdIns4P at the basis of microvilli basis. In other models, it has been shown that the PtdIns(4,5)P2 level determines the activation status of ERM proteins that participate in the process of the formation of microvilli and trigger a positive feedback cycle involving Rho-GTP, PIP5K, and PtdIns(4,5)P2 production.[17,19] Our results are thus consistent with a potential role for PtdIns(4,5)P2, p-ERM, and RhoA in this process, but other mechanisms could be responsible as well. The increased PtdIns(4,5)P2 substrate and decreased PtdIns4P product of SHIP2 observed in LLC-PK1 experiments, the facts that the $Ship2^{\Delta}$ allele leads to the production of a catalytically inactive Ship2 protein in $Ship2^{\Delta/\Delta}$ and in $Ship2^{flox/flox}$ mSglt2-Cre mice and that the SHIP2 catalytic inhibitor used in LLC-PK1 cell studies reproduced the alterations of microvilli observed *in vivo* in mice all support an important role of the SHIP2 catalytic activity in the microvillus phenotype. Surprisingly, no alterations of microvilli were detected in the intestinal microvilli of $Ship2^{\Delta/\Delta}$ mice compared with $Ship2^{+/+}$ mice, suggesting that the microvillus phenotype is specific for the kidney (data not shown). Interestingly, SHIP2 catalytic inactivation in our *in vivo* and *in vitro* models not only results in increased formation of microvilli and density on PT epithelial cells, but also in increased PT function. Indeed, reabsorption of LMWP, glucose, and phosphate as well as uptake of albumin by PT cells were all increased when the SHIP2 catalytic unit was inactivated. Urinary osmolarity, a measure of solute concentration, was found to be decreased in $Ship2^{flox/flox}$ mSglt2-Cre mice compared with control mice and probably also reflects the increased function of solute reabsorption by PT epithelium. Whether the increased reabsorption of LMWP and albumin observed when SHIP2 catalytic function is inactivated is solely due to the increased formation and density of microvilli on PT epithelial cells is unknown. Indeed, in COS-7 cells, SHIP2 is known to control PtdIns(4,5)P2 levels at clathrin-coated pit and clathrin-mediated endocytosis, a pivotal process during receptor-mediated reabsorption in PT cells.[21] Thus, the increased reabsorption of LMWP and albumin could result from combined increased density of microvilli and endocytosis in PT cells. By contrast, reabsorption of glucose and phosphates by PT cells does not implicate receptor-mediated endocytosis and the action of SHIP2 on this process. The increased PT cell function does not seem to be limited to reabsorption because urinary creatinine level, which is classically regarded as a marker of urine concentration, was increased in $Ship2^{flox/flox}$ mSglt2-Cre mice compared with control mice. This alteration may reflect increased creatinine secretion by this nephron segment.[22–24]

Figure 4 | Urine analysis in $Ship2^{flox/flox}$ mSglt2-Cre mice. (**a**) Urinary protein profile was analyzed in male (left panel) and female (right panel) 20-week-old $Ship2^{flox/flox}$ mSglt2-Cre mice and control mice. Urine volumes, normalized to total urinary protein levels, were loaded onto a nonreducing sodium dodecylsulfate polyacrylamide gel followed by staining with Coomassie blue. Urinary protein analysis showed decreased signals corresponding to proteins with a molecular weight <25 kDa in some male and female $Ship2^{flox/flox}$ mSglt2-Cre mice compared with control mice. Marker proteins are shown. (**b**) Quantification of the major protein signal at ~18 kDa was performed in males (graph on left) and females (graph on right) using ImageJ software. (**c**) Twenty-week-old mice (9–19 mice per genotype) were i.v. injected with 10 mg of fluorescein isothiocyanate (FITC)–albumin per kilogram of body weight. One hour after injection, fluorescence intensity was measured in urine and plasma, and the mean ± SEM of fluorescence intensity, normalized to urinary creatinine levels, was calculated. No fluorescence was detected in plasma and urine before the FITC-albumin injection. Fluorescence intensity in plasma was not significantly different in control and $Ship2^{flox/flox}$ mSglt2-Cre mice. (**d**) Fractional excretion of phosphate was calculated in $Ship2^{flox/flox}$ mSglt2-Cre and control mice. The mean ± SEM of 9 to 23 mice per genotype is shown. Fractional renal excretion of phosphate was significantly decreased in $Ship2^{flox/flox}$ mSglt2-Cre mice compared with control mice. Statistics (Student's *t* test): $^{*}P < 0.05$ compared with control mice. (**e**) Urinary osmolarity, normalized to urinary creatinine, was measured in $Ship2^{flox/flox}$ mSglt2-Cre and control mice. The mean ± SEM of 10 to 21 mice per genotype are shown. Urinary osmolarity was significantly decreased in $Ship2^{flox/flox}$ mSglt2-Cre mice compared with control mice. Statistics (Student's *t* test): $^{**}P < 0.01$ compared with control mice. (**f**) Twenty-week-old mice (6–8 per genotype) were i.p. injected with 2 g of glucose per kilogram of body weight. The mean ± SEM of glucose in blood (left panels) and urine (right panels) was analyzed over a 2- and a 4-hour period, respectively. The areas under the curve (AUC, lower panels) were determined using Graph Pad Prism software. To optimize viewing of this image, please see the online version of this article at www.kidney-international.org.

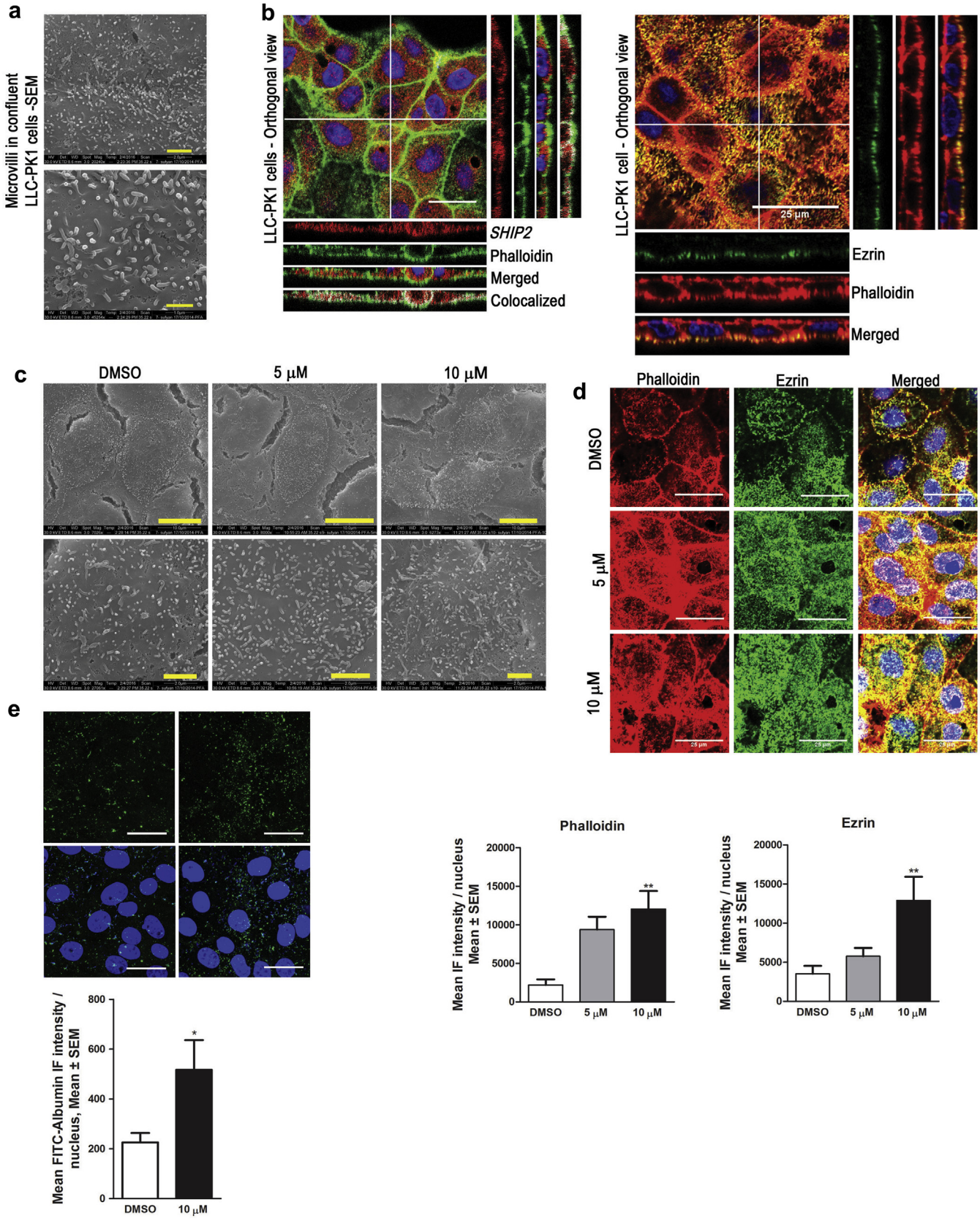
a
Microvilli in confluent LLC-PK1 cells -SEM
b
LLC-PK1 cells - Orthogonal view
SHIP2
Phalloidin
Merged
Colocalized
LLC-PK1 cell - Orthogonal view
25 µm
Ezrin
Phalloidin
Merged
c
DMSO
5 µM
10 µM
d
Phalloidin
Ezrin
Merged
DMSO
5 µM
10 µM
e
Mean FITC-Albumin IF intensity / nucleus, Mean ± SEM
800
600
400
200
0
*
DMSO
10 µM
Phalloidin
Mean IF intensity / nucleus Mean ± SEM
20000
15000
10000
5000
0
**
DMSO
5 µM
10 µM
Ezrin
Mean IF intensity / nucleus Mean ± SEM
20000
15000
10000
5000
0
**
DMSO
5 µM
10 µM

Renal Fanconi syndrome is characterized by impaired solute and protein reabsorption by PT.[1,2] In addition to rare inherited disorders such as Lowe syndrome and Dent's disease, many conditions may lead to a renal Fanconi syndrome: multiple myeloma, autoimmune syndromes (e.g., Sjögren syndrome), administration of drugs (e.g., aminoglycosides, valproate, ifosfamide, tenofovir), ischemic injury, and intoxication by heavy metals (e.g., lead, mercury). These conditions are associated with a loss of the brush border on PT cells (ischemic injury[25]), a selective loss of megalin and cubilin at the brush border (Dent's disease[26]), altered PT endocytosis (Lowe syndrome and Dent's disease), and sometimes PT epithelial repair and regeneration (drugs, ischemic injury, and heavy metal intoxication[27]). It will be interesting to investigate whether the SHIP2 catalytic inhibitor used in this study is able to fully or partially restore normal PT reabsorption function in animal models of selected renal Fanconi syndromes by increasing PT microvilli formation and density.

MATERIALS AND METHODS

Mice

Ship2$^{\Delta/+}$ and *Ship2*$^{flox/+}$ mice were generated on a mixed 129 × C57BL/6 genetic background in our laboratory.[10] *Ship2*$^{\Delta/\Delta}$ mice have *Ship2* exons 18 and 19 deleted but still express a truncated and catalytically inactive SHIP2 protein. Mice with a *Ship*2 mutation specifically in kidney PT (*Ship2*$^{flox/flox}$ mSglt2-Cre mice) were generated by crossing our Ship2$^{flox(18+19)/+}$ mice with mSglt2-Cre mice.[9] All mice were housed in an animal facility with 12-hour light/12-hour dark cycles and had free access to food and water throughout the study period unless otherwise mentioned. All mouse studies were authorized by the Animal Care Use and Review Committee of the University of Liège.

Pig LLC-PK1 (ATCC CL-101) PT cell culture, treatment, transduction, and transfection

LLC-PK1 cells were cultured at confluency in MEM alpha media (Gibco #12571063, Thermo Fisher Scientific, Waltham, MA) supplemented with 10% heat inactivated fetal bovine serum (Gibco #16140071), penicillin-streptomycin (Gibco #15070063), and 2 mM L-glutamine (Gibco #25030081). For small-molecule SHIP2 inhibitor treatment, LLC-PK1 cells were grown over collagen-coated 12-mm glass coverslips for 5 days in culture medium. Then the culture medium was replaced by fresh media containing either DMSO or SHIP2 inhibitor (5 or 10 μM), and the cells were incubated for another 2 days. At the end of the treatment period, cells were washed and fixed with 10% formalin solution. LLC-PK1 cells were transduced (150 viruses per cell) with lentivirus particles expressing GFP, a puromycin resistance cassette, and either siRNA targeted against pig *Ship2/Inppl1* or a scrambled RNA sequence as control (all obtained from ABM Inc, Richmond, Canada). Four pig *Ship2* siRNA sequences were used in the study: siRNA1 (5′-ATCCA GGAGATCCTCAACTACATCAGCCG-3′), siRNA2 (5′-CCA CATCATCTGCAACTCCTACGGCTGCA-3′), siRNA3 (5′-CGCAC TAAGTTCTTCATTGAGTTCTACTC-3′), and siRNA4 (5′-CCACTGTCGAAGTTATTTGAGGAACCAGA-3′). Seventy-two hours after transduction, cells were incubated with puromycin (1 μg/ml) for 2 days. Puromycin-resistant cells were grown over glass coverslips for immunofluorescence or in 6-well plates for immunodetection. LLC-PK1 cells were also transfected with a Myc-tagged PIP5K1b expression plasmid using Lipofectamine-2000 (#12566014, Invitrogen, Carlsbad, CA), according to J. Ikenouchi.[19] Twenty-four hours after the transfection, media were replaced with fresh media containing either DMSO or SHIP2 inhibitor (5 or 10 μM), and cells were cultured for 2 days, washed, and fixed. After that, IF staining was performed as described in the following.

GFR measurement

The GFR was assessed by plasma clearance of FITC-labeled inulin injected i.v. as a single bolus using the protocol described by Rieg.[28] Briefly, mice were injected i.v. with FITC-labeled inulin (40 μg/g of body weight), and blood samples from the tail were collected at 3, 5, 7, 10, 15, 35, 56, and 75 minutes post-injection. Plasma samples were obtained by centrifugation, and the mean fluorescence intensity was measured using a fluorescence detector (EnSpire plate reader, PerkinElmer, Waltham, MA). Two-phase exponential decay curve fitting was performed using Prism software (GraphPad Software Inc., La Jolla, CA), and the GFR was calculated: GFR = n/(A/K1 + B/K2), where n = injected amount (n = C × V, where C = FITC-inulin concentration, V = injected volume), A = SPAN1, *y*-intercept of elimination,

Figure 5 | Pharmacologic inactivation of SHIP2 in the pig LLC-PK1 proximal tubule cell line confirms structural, ultrastructural, and functional alterations observed in *Ship2*$^{\Delta/\Delta}$ and *Ship2*$^{flox/flox}$ mSglt2-Cre proximal tubules. (**a**) SEM analysis of confluent LLC-PK1 cells showing microvilli. Bars = 2 μm in the top image and 1 μm in the bottom image. (**b**) Immunofluorescence (IF) analysis of confluent LLC-PK1 cell cultures showing SHIP2 expression (red) in the cytoplasm up to and sometimes including the basis of phalloidin-positive (green) microvilli (left panel). White dots show areas of colocalization of SHIP2 and phalloidin at the base of microvilli. The right panel shows the colocalization of microvilli phalloidin (red) and ezrin (green) expression. Nuclei are stained with 4′,6-diamidino-2-phenylindole (DAPI) (blue). Orthogonal projections along the white lines are shown. Bars = 25 μm. (**c**) SEM analyses of confluent LLC-PK1 cells treated with 5 or 10 μM SHIP2 catalytic inhibitor or with dimethylsulfoxide (DMSO) as control. Treatment with the SHIP2 catalytic inhibitor resulted in increased microvilli density. Bars = 10 μm in the upper panels and 2 μm in the lower panels. (**d**) Microvilli phalloidin (red) and ezrin (green) IF analysis in confluent LLC-PK1 cells treated with 5 or 10 μM SHIP2 catalytic inhibitor or with DMSO as a control. Nuclei are stained with DAPI (blue). Bars = 25 μm. Graphs represent the quantification of the microvilli phalloidin and ezrin signals. Mean IF intensities per nucleus ± SEM are shown; 50 to 100 LLC-PK1 cells were analyzed for quantification. Microvilli phalloidin and ezrin expression were significantly increased in SHIP2 catalytic inhibitor–treated LLC-PK1 cell cultures compared with DMSO-treated cell cultures. Statistics (1-way analysis of variance): $^{**}P < 0.01$ compared with DMSO-treated LLC-PK1 cell cultures. (**e**) Confluent LLC-PK1 cells were treated with 10 μM SHIP2 catalytic inhibitor or with DMSO as a control and incubated with 100 mg fluorescein isothiocyanate (FITC)-albumin (green) per liter of culture medium for 1 hour and then processed for FITC-albumin uptake analysis. Nuclei were stained with DAPI (blue). Bars = 25 μm. The graph represents the quantification of the FITC-albumin signal; the mean IF intensities per nucleus ± SEM are shown. FITC-albumin uptake by microvilli from confluent LLC-PK1 cell culture was significantly increased in the presence of 10 μM SHIP2 catalytic inhibitor compared with DMSO-treated LLC-PK1 cells. Statistics (Student's *t* test): $^{*}P < 0.05$ compared with DMSO-treated LLC-PK1 cells. To optimize viewing of this image, please see the online version of this article at www.kidney-international.org.

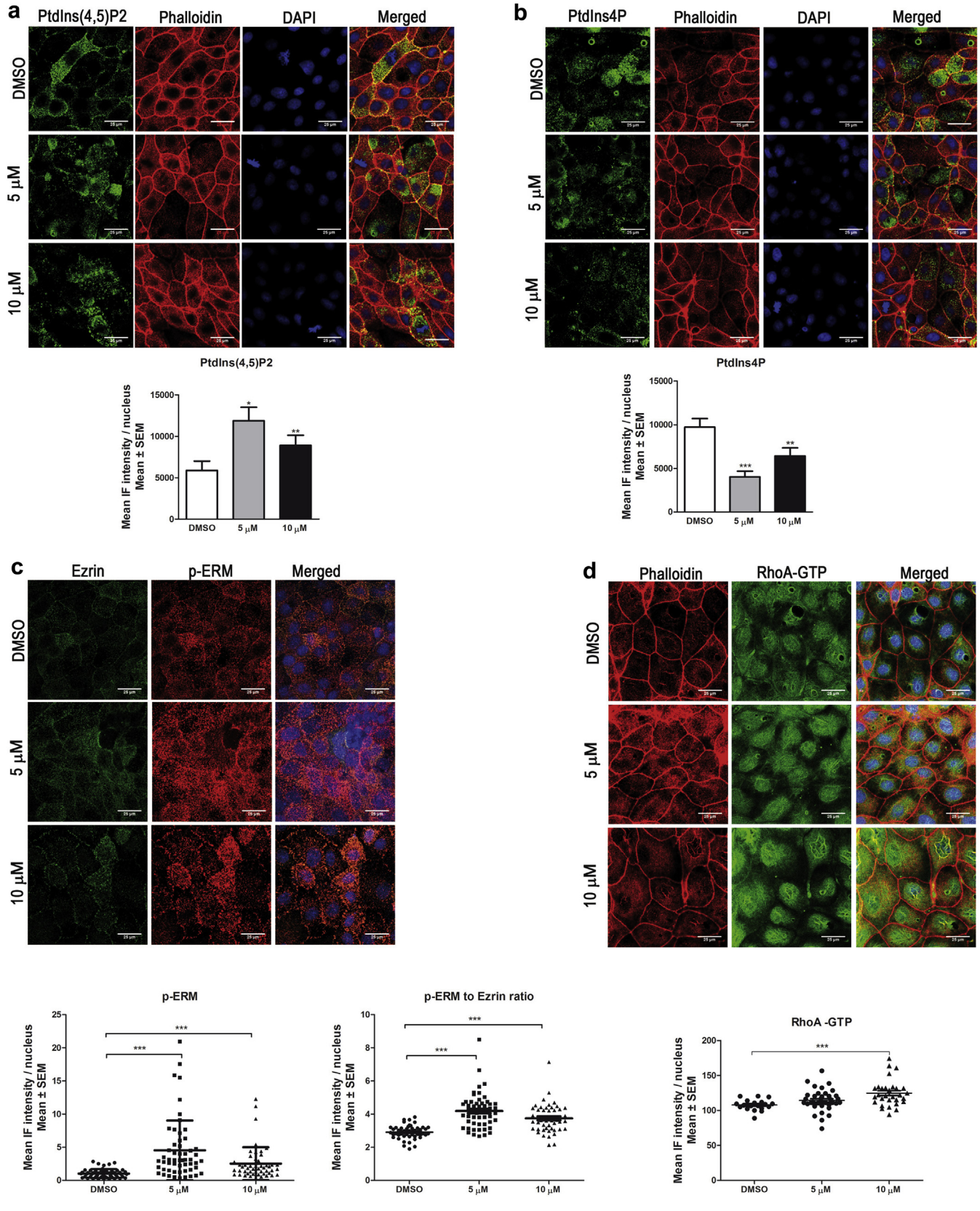
a
PtdIns(4,5)P2
Phalloidin
DAPI
Merged
DMSO
5 μM
10 μM
PtdIns(4,5)P2
Mean IF intensity / nucleus
Mean ± SEM
15000
10000
5000
0
*
**
DMSO
5 μM
10 μM
b
PtdIns4P
Phalloidin
DAPI
Merged
DMSO
5 μM
10 μM
PtdIns4P
Mean IF intensity / nucleus
Mean ± SEM
15000
10000
5000
0
***
**
DMSO
5 μM
10 μM
c
Ezrin
p-ERM
Merged
DMSO
5 μM
10 μM
d
Phalloidin
RhoA-GTP
Merged
DMSO
5 μM
10 μM
p-ERM
Mean IF intensity / nucleus
Mean ± SEM
25
20
15
10
5
0
***
***
DMSO
5 μM
10 μM
p-ERM to Ezrin ratio
Mean IF intensity / nucleus
Mean ± SEM
10
8
6
4
2
***
***
DMSO
5 μM
10 μM
RhoA -GTP
Mean IF intensity / nucleus
Mean ± SEM
200
150
100
50
0
***
DMSO
5 μM
10 μM

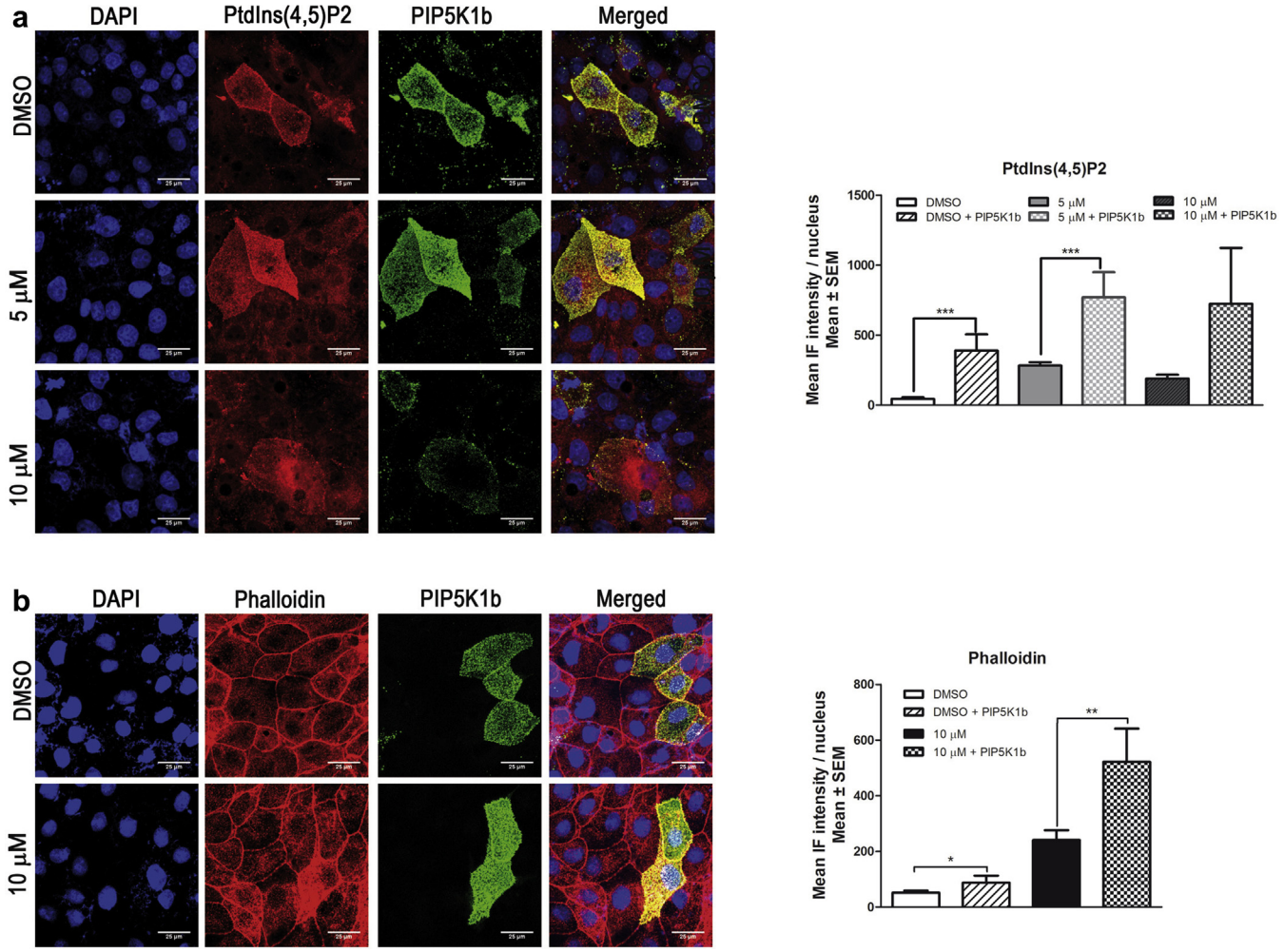

Figure 7 | Effect of PIP5K1b overexpression on PtdIns(4,5)P2 level and microvilli formation in LLC-PK1 cells treated or not with the SHIP2 catalytic inhibitor. Immunofluorescence (IF) on confluent LLC-PK1 cells transfected with Myc-tagged (green) PIP5K1b followed by treatment with 5 or 10 μM SHIP2 catalytic inhibitor or dimethylsulfoxide (DMSO) as a control. Plasma membrane/microvilli PtdIns(4,5)P2 (red, **a**) and phalloidin (red, **b**) expression is shown. Nuclei are stained with 4′,6-diamidino-2-phenylindole (DAPI) (blue). Bars = 25 μm. Graphs represent the quantification of the PtdIns(4,5)P2 (**a**) and the phalloidin (**b**) signals; mean pixel intensities per nucleus ± SEM are shown. Plasma membrane/microvilli PtdIns(4,5)P2 level and phalloidin signal were further increased in SHIP2 inhibitor–treated LLC-PK1 cells transfected with PIP5K1b compared with neighboring nontransfected SHIP2 catalytic inhibitor–treated LLC-PK1 cells. Statistics (Student's *t* test): $^{*}P < 0.05$, $^{**}P < 0.01$, and $^{***}P < 0.001$. To optimize viewing of this image, please see the online version of this article at www.kidney-international.org.

K1 = decay constant for elimination, B = SPAN2, *y*-intercept of distribution, and K2 = decay constant for distribution.[28]

Statistics

All data are expressed as mean ± SEM. Statistical significance was determined using Student's *t* test for comparison of 2 independent groups. $P < 0.05$ was considered statistically significant. All statistical analyses were performed using GraphPad Prism software (GraphPad Software Inc.).

DISCLOSURE

All the authors declared no competing interests.

AUTHOR CONTRIBUTION

SGS proposed the project on the analysis of the kidney in *Ship2*$^{\Delta/\Delta}$ mice, performed most experiments, discussed the results, and helped with the writing of the manuscript. DP-M and MV performed SEM and TEM experiments on kidney and LLC-PK1 cells, discussed the results, and reviewed the manuscript. FJ discussed experiments and results

Figure 6 | Altered PtdIns(4,5)P2 substrate, PtdIns4P product, phospho-ezrin/radixin/moesin (p-ERM), and RhoA-GTP levels in LLC-PK1 cells after pharmacologic inactivation of SHIP2. Immunofluorescence (IF) analysis of confluent LLC-PK1 cells treated with 5 or 10 μM SHIP2 catalytic inhibitor or with dimethylsulfoxide (DMSO) (as a control) showing plasma membrane/microvilli PtdIns(4,5)P2 (**a**, green), PtdIns4P (**b**, green), microvilli p-ERM proteins (**c**, red), and RhoA-GTP (**d**, green) expressions. Nuclei are stained with 4′,6-diamidino-2-phenylindole (DAPI) (blue). Bars = 25 μm. Graphs represent the quantification of PtdIns(4,5)P2, PtdIns4P, p-ERM proteins, and RhoA-GTP signals; mean pixel intensities per nucleus ± SEM are shown; 50 to 100 cells were analyzed for quantification; each dot represents a LLC-PK1 cell. The ratio of p-ERM signal to ezrin signal is also presented. Statistics (one-way analysis of variance): $^{*}P < 0.05$, $^{**}P < 0.01$, and $^{***}P < 0.001$ compared with DMSO-treated LLC-PK1 cells. To optimize viewing of this image, please see the online version of this article at www.kidney-international.org.

and reviewed the manuscript. SS supervised the project, brought financial support, discussed the results, and wrote the manuscript.

ACKNOWLEDGMENTS

We thank Christophe Erneux (Université Libre de Bruxelles, Brussels, Belgium) for the SHIP2 antibody, Michael Caplan (Yale University, New Haven, CT, USA) for LLC-PK1 cells, Isabelle Rubera (Université de Nice Sophia Antipolis, Nice, France) for mSglt2-Cre mice, Laoura Sacré and Aurore Cue Alvarez (Laboratoire de Génétique Fonctionnelle, GIGA Research Centre) for technical help, Junichi Ikenouchi (Kyoto University, Kyoto, Japan) for Myc-tagged PIP5K1b expression plasmid, and the GIGA technology platforms (mouse facility, imaging, viral vectors, and immunohistology). This work was supported by a Crédit de Recherches grant (CDR #J.0021.16/26035539) obtained by S. S. from the Fonds de la recherché Scientifique (FRS-FNRS, Belgium). The CMMI is supported by the European Regional Development Fund and Wallonia.

SUPPLEMENTARY MATERIAL

Supplementary Materials and Methods.

Figure S1. The SHIP2 protein is expressed in the mouse renal proximal tubule (PT). (**A**) Immunodetection with SHIP2 and tubulin antibodies on kidney protein extracts isolated from 3 *Ship2*$^{+/+}$ mice. Immunofluorescence analysis of SHIP2 (red) and phalloidin (green) (**B**) or SHIP2 (red) and megalin (green) (**C,D**) expression on kidney sections from a *Ship2*$^{+/+}$ mouse. In (**D**), the SHIP2 signal is detected on transverse and longitudinal sections of megalin-positive PT cells, but it did not overlap with the megalin signal, indicating that SHIP2 is expressed in PT cells, but not within the brush border. DAPI, 4′,6-diamidino-2-phenylindole. Bars = 50 μm (**B** and **C**) and 25 μm (**D**).

Figure S2. Histologic analysis of *Ship2*$^{+/+}$ and *Ship2*$^{\Delta/\Delta}$ kidneys. Kidney sections (5 μm) from 20-week-old female (**A**) and male (**B**) mice were analyzed after hematoxylin and eosin staining. No obvious alteration was detected in *Ship2*$^{\Delta/\Delta}$ mice compared with *Ship2*$^{+/+}$ mice. Bars = 50 μm. (**C**) Total numbers of glomeruli were counted in the whole transversal kidney sections in at least 3 mice of each genotype (graph on left). The total numbers of tubules per square millimeter were counted in the whole kidney sections (graph on right). No significant difference was observed in total number of glomeruli or tubules counted in *Ship2*$^{\Delta/\Delta}$ mice compared with *Ship2*$^{+/+}$ mice.

Figure S3. Effect of SHIP2 catalytic inactivation on mRNA expression level of genes coding for transporters mainly expressed in the brush border versus the basolateral membrane of the kidney proximal tubule (PT) cell. Level of mRNA expression was determined in *Ship2*$^{\Delta/\Delta}$ and *Ship2*$^{+/+}$ kidneys using quantitative reverse transcriptase polymerase chain reaction. Graphs show the ratio of Ct values for each gene with glyceraldehyde-3-phosphate dehydrogenase as the fold change compared with *Ship2*$^{+/+}$ kidney. Means ± SEM are presented. Expression levels of mRNA coding for megalin, cubilin, Sglt2, and Clcn5, all proteins expressed in the PT brush border, were significantly increased in *Ship2*$^{\Delta/\Delta}$ kidney compared with *Ship2*$^{+/+}$ kidney. Statistics (Student's *t* test): $^{*}P < 0.05$.

Figure S4. Effect of SHIP2 catalytic inactivation on microvilli thickness in proximal tubules of *Ship2*$^{+/+}$ and *Ship2*$^{\Delta/\Delta}$ kidneys. The graph represents the thickness of microvilli measured on transmission electron microscopy images from *Ship2*$^{+/+}$ and *Ship2*$^{\Delta/\Delta}$ kidney sections. No significant difference was observed between the thickness of microvilli in *Ship2*$^{+/+}$ and *Ship2*$^{\Delta/\Delta}$ proximal tubules.

Figure S5. SHIP2 immunofluorescence (IF) analysis in control and *Ship2*$^{flox/flox}$ mSglt2-Cre kidney sections. IF analysis of *Ship2*$^{flox/flox}$ mSglt2-Cre and control kidney sections with a SHIP2 antibody (green) and phalloidin (red). Bars = 50 μm. G, glomerulus; PT, proximal tubule. As expected, the SHIP2 signal is still present in phalloidin-positive PT cells from *Ship2*$^{flox/flox}$ mSglt2-Cre mice, but somewhat decreased compared with phalloidin-positive PTs of control kidney. Indeed, in our *Ship2* genetically modified mouse, the *Ship2*$^{\Delta}$ allele still produces a slightly unstable, catalytically inactive, truncated SHIP2 protein that is recognized by the SHIP2 antibody.[10]

Figure S6. Macroscopic, structural, and ultrastructural analysis of *Ship2*$^{flox/flox}$ mSglt2-Cre and control mice. (**A**) No facial or length dysmorphy was observed in 20-week-old *Ship2*$^{flox/flox}$ mSglt2-Cre mice compared with control mice. (**B**) Kidney sections (5 μm) from 20-week-old *Ship2*$^{flox/flox}$ mSglt2-Cre and control mice were analyzed after hematoxylin and eosin staining. No obvious alteration was detected in *Ship2*$^{flox/flox}$ mSglt2-Cre mice compared with control mice. In particular, glomeruli and tubule density, size, and localization as well as general structure of the kidney were found normal; no cyst or interstitial alterations, including cell infiltrate, were detected in *Ship2*$^{flox/flox}$ mSglt2-Cre kidneys. Bars = 50 μm. (**C**) SEM analysis in *Ship2*$^{flox/flox}$ mSglt2-Cre mice also revealed proximal tubule (PT) and brush borders with only very slight alterations compared with control mice. Bars = 10 μm.

Figure S7. Phalloidin staining in confluent LLC-PK1 cell cultures. Immunofluorescence (IF) analysis of confluent LLC-PK1 cell cultures showing total (upper panel), top of cell (center panel, where microvilli are present), and bottom of cell (lower panel where actin stress fibers are located) phalloidin expression (red). The dotted pattern of phalloidin staining at the top of LLC-PK1 cells represents microvilli. Nuclei are stained with 4′,6-diamidino-2-phenylindole (DAPI) (blue). Bars = 25 μm.

Figure S8. Megalin expression and fluorescein isothiocyanate (FITC)–albumin uptake by microvilli in confluent LLC-PK1 cells treated with a SHIP2 catalytic inhibitor. (**A**) Confluent LLC-PK1 cells were treated with 5 or 10 μM SHIP2 catalytic inhibitor or with dimethylsulfoxide (DMSO) as a control and analyzed for megalin (green) and phalloidin (red) expression. Nuclei were stained with 4′,6-diamidino-2-phenylindole (DAPI) (blue). Bars = 25 μm. Graphs represent the quantification of the microvilli phalloidin and megalin signals. Mean immunofluorescence (IF) intensities per nucleus ± SEM are shown. For quantification, 50 to 100 cells were analyzed per group. Statistics (1-way analysis of variance): $^{***}P < 0.001$ compared with DMSO-treated LLC-PK1 cell cultures. (**B**) Confluent LLC-PK1 cells were treated with 10 μM SHIP2 catalytic inhibitor and incubated with 100 mg FITC-albumin (green) per liter of culture medium. One hour after addition, FITC-albumin is mainly localized in phalloidin-positive microvilli of confluent LLC-PK1 cells. Nuclei were stained with DAPI (blue). Bars = 25 μm.

Figure S9. SHIP2 expression in LLC-PK1 cells transduced with lentivirus expressing *Ship2*-specific small, interfering RNAs (siRNAs). (**A**) SHIP2 and vinculin Western blotting on protein extracts isolated from LLC-PK1 cells transduced with lentivirus expressing either scrambled (Sc) or SHIP2-specific (1, 2, 3, and 4) siRNAs. (**B**) Quantification of the SHIP2 signal, normalized to the vinculin signal and reported as the percentage of scrambled RNA results.

Figure S10. Immunofluorescence (IF) analysis of microvilli phalloidin, phospho ezrin/radixin/moesin (p-ERM) proteins, and PtdIns(4,5)P2 expression in LLC-PK1 cells transduced with lentivirus expressing *Ship2*-specific small, interfering RNAs (siRNAs). Confluent LLC-PK1 cells were transduced with lentivirus expressing either scrambled RNA (sc RNA) or *Ship2*-specific (1, 2, 3, and 4) siRNAs and analyzed (**A**) for phalloidin (red), phospho-ERM proteins (magenta), and lentiviral enhanced green fluorescent protein (eGFP) (green)) or for (**C**) PtdIns(4,5)P2 (red) and lentiviral eGFP (green). Nuclei are stained with 4′,6-diamidino-2-phenylindole (DAPI) (blue). Bars = 25 μm. Graphs represent the quantification of microvilli phalloidin and phospho-ERM protein signals (**B**) or PtdIns(4,5)P2 signals (**D**). Mean IF intensities per nucleus ± SEM are shown. For quantification, 50 to 100 cells were analyzed per group. Statistics (1-way analysis of variance): $^{*}P < 0.05$, $^{**}P < 0.01$, and $^{***}P < 0.001$ compared with LLC-PK1 cell cultures transduced with scrambled siRNA expressing lentivirus.

Figure S11. Increased phospho ezrin/radixin/moesin (p-ERM) signal in *Ship2*$^{\Delta/\Delta}$ kidney. Immunodetection of p-ERM and vinculin by Western blotting on kidney protein extracts isolated from *Ship2*$^{+/+}$ and *Ship2*$^{\Delta/\Delta}$ mice. A stronger p-ERM signal is observed in *Ship2*$^{\Delta/\Delta}$ mice than in *Ship2*$^{+/+}$ mice, supporting the immunofluorescence results obtained in LLC-PK1 cells treated with the SHIP2 catalytic inhibitor.

Table S1. Body and kidney weights, glomerular filtration rate (GFR), and plasma creatinine levels in *Ship2*$^{+/+}$ and *Ship2*$^{\Delta/\Delta}$ mice.

Table S2. List of primer sequences used for quantitative reverse-transcriptase polymerase chain reaction.

Table S3. Body and kidney weights, glomerular filtration rate (GFR), and creatinine levels in *Ship2*$^{flox/flox}$ mSglt2-Cre and control mice.

Supplementary material is linked to the online version of the paper at www.kidney-international.org.

REFERENCES

1. Bergeron M, Gougoux A, Vinay P. The renal Fanconi syndrome. In: Sciver R, Beudet AL, Sly WS, Valle D, eds. *The Metabolic and Molecular Basis of Inherited Diseases*. New York, NY: McGraw-Hill; 1995: 3691–3704.
2. Harrison HE. The Fanconi syndrome. *J Chron Dis*. 1953;7:346–355.
3. van't Hoff WG. Biology and genetics of inherited renal tubular disorders. *Exp. Nephrol*. 1996;4:253–262.
4. Schurmans S, Carrió R, Behrends J, et al. The mouse SHIP2 (Inppl1) gene: complementary DNA, genomic structure, promoter analysis, and gene expression in the embryo and adult mouse. *Genomics*. 1999;62: 260–271.
5. Muraille E, Dassesse D, Vanderwinden JM, et al. The SH2 domain-containing 5-phosphatase SHIP2 is expressed in the germinal layers of embryo and adult mouse brain: increased expression in N-CAM-deficient mice. *Neuroscience*. 2001;105:1019–1030.
6. Bacchini A, Gaetani E, Cavaggioni A. Pheromone binding proteins of the mouse, Mus musculus. *Experientia*. 1992;48:419–421.
7. Böcskei Z, Groom CR, Flower DR, et al. Pheromone binding to two rodent urinary proteins revealed by X-ray crystallography. *Nature*. 1992;360: 186–188.
8. Pelosi P, Mastrogiacomo R, Iovinella I, et al. Structure and biotechnological applications of odorant-binding proteins. *Appl Microbiol Biotechnol*. 2014;98:61–70.
9. Rubera I, Poujeol C, Bertin G, et al. Specific Cre/lox recombination in the mouse proximal tubule. *J Am Soc Nephrol*. 2004;15:2050–2056.
10. Dubois E, Jacoby M, Blockmans M, et al. Developmental defects and rescue from glucose intolerance of a catalytically-inactive novel Ship2 mutant mouse. *Cell Signal*. 2012;24:1971–1980.
11. Mulli JM, Weibel J, Diamond L, et al. Sugar transport in the LLC-PK1 renal epithelial cell line: similarity to mammalian kidney and the influence of cell density. *J Cell Physiol*. 1980;104:375–389.
12. Loomis PA, Zheng L, Sekerková G, et al. Espin cross-links cause the elongation of microvillus-type parallel actin bundles in vivo. *J Cell Biol*. 2003;163:1045–1055.
13. Hirao M, Sato N, Kondo T, et al. Regulation mechanism of ERM (ezrin/radixin/moesin) protein/plasma membrane association: possible involvement of phosphatidylinositol turnover and Rho-dependent signaling pathway. *J Cell Biol*. 1996;135:37–51.
14. Barret C, Roy C, Montcourrier P, et al. Mutagenesis of the phosphatidylinositol 4,5-bisphosphate (PIP(2)) binding site in the NH(2)-terminal domain of ezrin correlates with its altered cellular distribution. *J Cell Biol*. 2000;151: 1067–1080.
15. Niggli V, Andréoli C, Mangeat P. Identification of a phosphatidylinositol-4,5-bisphosphate-binding domain in the N-terminal region of ezrin. *FEBS Lett*. 1995;376:172–176.
16. Matsui T, Yonemura S, Tsukita S, et al. Activation of ERM proteins in vivo by Rho involves phosphatidyl-inositol 4-phosphate 5-kinase and not ROCK kinases. *Curr Biol*. 1999;9:1259–1262.
17. Tsukita S, Yonemura S. Cortical actin organization: lessons from ERM (Ezrin/Radixin/Moesin) proteins. *J Biol Chem*. 1999;274:34507–34510.
18. Yonemura S, Matsui T, Tsukita S, et al. Rho-dependent and –independent activation mechanisms of ezrin/radixin/moesin proteins: an essential role for polyphosphoinositides in vivo. *J Cell Sci*. 2002;115:2569–2580.
19. Bretscher A. Regulation of cortical structure by the ezrin-radixin-moesin protein family. *Curr Opin Cell Biol*. 1999;11:109–116.
20. Ikenouchi J, Hirata M, Yonemura S, et al. Sphingomyelin clustering is essential for the formation of microvilli. *J Cell Sci*. 2013;126:3585–3592.
21. Nakatsu F, Perera RM, Lucast L, et al. The inositol 5-phosphatase SHIP2 regulates endocytic clathrin-coated pit dynamics. *J Cell Biol*. 2010;190: 307–315.
22. Eisner C, Faulhaber-Walter R, Wang Y, et al. Major contribution of tubular secretion to creatinine clearance in mice. *Kidney Int*. 2010;77:519–526.
23. Vallon V, Eraly SA, Rao SR, et al. A role for the organic anion transporter OAT3 in renal creatinine secretion in mice. *Am J Physiol Renal Physiol*. 2012;302:1293–1299.
24. Breyer MD, Qi Z. Better nephrology for mice–and man. *Kidney Int*. 2010;77:487–489.
25. Sharfuddin AA, Molitoris BA. Pathophysiology of ischemic acute kidney injury. *Nat Rev Nephrol*. 2011;7:189–200.
26. Christensen EI, Devuyst O, Dom G, et al. Loss of chloride channel ClC-5 impairs endocytosis by defective trafficking of megalin and cubilin in kidney proximal tubules. *Proc Natl Acad Sci U S A*. 2003;100:8472–8477.
27. Berger K, Moeller MJ. Mechanisms of epithelial repair and regeneration after acute kidney injury. *Semin Nephrol*. 2014;34:394–403.
28. Rieg T. A high-throughput method for measurement of glomerular filtration rate in conscious mice. *J Vis Exp*. 2013;75:e50330.